INSTITUTE OF PHYSICS PUBLISHING JOURNAL OF PHYSICS D: APPLIED PHYSICS

J. Phys. D: Appl. Phys. **38** (2005) 872–876 doi:10.1088/0022-3727/38/6/015

Electron drift velocity in NH_3 in strong electric fields determined from rf breakdown curves

V Lisovskiy[1,3], S Martins[2], K Landry[2], D Douai[2], J-P Booth[1] and V Cassagne[2]

[1] Laboratoire de Physique et Technologie des Plasmas, Ecole Polytechnique, Palaiseau 91128, France
[2] Unaxis Displays Division France SAS, 5, Rue Leon Blum, Palaiseau 91120, France
[3] Department of Physics and Technology, Kharkov National University, Kharkov 61077, Ukraine

E-mail: lisovskiy@yahoo.com

Received 29 November 2004, in final form 13 January 2005
Published 3 March 2005
Online at stacks.iop.org/JPhysD/38/872

Abstract
We report measurements of the breakdown curves of a radio-frequency capacitive discharge in low pressure ammonia. The electron drift velocity was determined from the location of turning points in the breakdown curves in the range of $E/p = 42$–$713\,\mathrm{V\,cm^{-1}\,Torr^{-1}}$. We compare our results to values calculated from the published cross-sections in the range $E/p = 1$–$5000\,\mathrm{V\,cm^{-1}\,Torr^{-1}}$ and find good agreement.

1. Introduction

Ammonia is widely used in various plasma-processing technologies. Radio-frequency (rf) discharges in ammonia are used to harden machine tools by nitriding [1] and to create protective coatings. Discharges in NH_3 are used for modifying the surface of SiO_2 films [2]. Mixtures of NH_3 with CO (or CO_2) are used to etch magnetic materials [3]. Ammonia is widely used for depositing silicon nitride films (in mixtures with silane SiH_4 [4–15], SiH_2Cl_2 [16] or $SiCl_4$ [17]). Therefore the breakdown characteristics of discharges in ammonia are of considerable interest.

Numerical simulation is often used to improve the understanding of processes taking place in the gas discharges. In order to use fluid simulations it is necessary to know the electron transport parameters (electron drift velocity V_{dr}, the first Townsend coefficient, α, the rate of electron attachment to gas molecules, η, electron diffusion coefficient, D_e) of the gas under study. To our knowledge, these transport parameters have only been measured in ammonia for moderate values of the reduced electric field, $E/p < 20\,\mathrm{V\,cm^{-1}\,Torr^{-1}}$ [18–21]; the average electron energy and the electron diffusion coefficient are given by Christophorou and Carter [22], who also give the energy lost in low-energy (<1.7 eV) collisions. However, the reduced field, E/p, may reach tens or hundreds of $\mathrm{V\,cm^{-1}\,Torr^{-1}}$ in the near-electrode sheaths of rf discharges, in the cathode sheath of dc discharges, during gas breakdown and in a number of other cases. In these conditions the electrons can acquire considerable energy, and therefore it is necessary to know the electron transport parameters in these strong electric fields.

The electron drift velocity in an electric field, V_{dr}, characterizes the conductivity of a weakly ionized gas and is one of the most important electron transport parameters. There are a number of techniques (the time-of-flight technique, observation of the optical radiation of a moving electron swarm, the shutter technique and so on) that have been used to measure the electron drift velocity. However, they only work for comparatively small reduced fields, E/p, because at higher values a self-sustaining discharge is ignited which impedes the measurement. The authors of papers [23–26] have proposed a novel method for determining the electron drift velocity from the location of the turning point in the breakdown curves of rf capacitive discharges. Whereas conventional techniques become inapplicable after the ignition of the self-sustaining discharge, this method is actually based on discharge ignition, allowing measurements of V_{dr} in strong electric fields.

In this paper we have used this technique to determine the electron drift velocity in ammonia. Measurements were made in the range $E/p = 42$–$713\,\mathrm{V\,cm^{-1}\,Torr^{-1}}$. With the help of the 'Bolsig' numerical code and published cross-sections [27] we have calculated the electron transport parameters in

ammonia in the range $E/p = 1$–$5000\,\mathrm{V\,cm^{-1}\,Torr^{-1}}$, and the drift velocity values obtained from our experiment agree well with the calculated values.

2. Experimental device

The rf discharge was ignited in NH_3 over the pressure range $p \approx 0.04$–30 Torr with an rf field frequency $f = \omega/2\pi = 13.56$ MHz. The distance between the flat circular aluminium electrodes (143 mm in diameter) was varied over the range $L = 2.5$–27 mm. The rf voltage (amplitude $U_{\mathrm{rf}} < 1300$ V) was fed to one of the electrodes, while the other was grounded. The electrodes were located inside a fused silica tube with an inner diameter of 145 mm. The gas was supplied through small orifices in the powered electrode and then pumped out via the gap between the second electrode and the wall of the fused silica tube.

The gas pressure was monitored with 10 and 1000 Torr capacitive manometers (MKS Instruments). The gas flow was fixed with a mass flow controller to 5 sccm, and the pressure regulated by throttling the outlet to the pump. The rf voltage was measured with an rf probe (Advanced Energy Z'SCAN).

We used the technique proposed by Levitskii [28] to measure the breakdown curves of the rf discharge. Near and to the high-pressure side of the minimum in the breakdown curve the ammonia pressure was fixed before slowly increasing the rf voltage until gas breakdown occurs. To the low-pressure side of the minimum the curve may be multi-valued, i.e. the curve turns around and breakdown occurs at two different values of the rf voltage. Therefore in this range we first decreased the ammonia pressure, then fixed the rf voltage value and only then increased the ammonia pressure slowly until discharge ignition occurred. At the moment of discharge ignition the rf voltage shows a sharp decrease, and a glow appears between the electrodes serving as a criterion for the onset of gas breakdown. The uncertainty in the measured breakdown voltages did not exceed 1–2 V over the whole U_{rf} range under study.

3. Experimental results

The breakdown curves of rf capacitive discharges can be divided into different branches according to the processes by which the charged particles are generated: emission-free, diffusion–drift, Paschen and multipactor branches [25]. A detailed description of the processes occurring in each of these branches is given elsewhere [25]. Figure 1 shows the experimental breakdown curves for an rf discharge in ammonia for a range of inter-electrode gap values. Consider the curve with a gap $L = 25$ mm. The Paschen branch occurs for $U_{\mathrm{rf}} > 300$ V. The diffusion–drift branch is well pronounced at $U_{\mathrm{rf}} < 300$ V. The emission-free branch occurs for $p > 1$ Torr. The multipactor branch was not observed at this large gap value, as it will occur at much higher rf voltage values (of the order of several thousand volts).

As is clear from figure 1, the breakdown curve for this gap possesses a region of multi-valued dependence of the rf breakdown voltage on gas pressure, i.e. the rf discharge can be ignited at two or even three different rf voltage values corresponding to the same gas pressure. For example, at a pressure of 0.1 Torr breakdown can occur at three voltages,

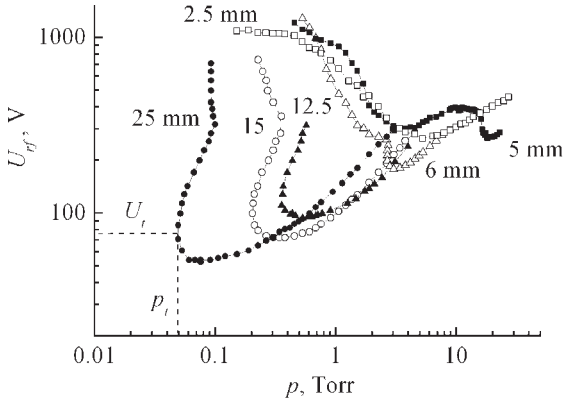

Figure 1. RF discharge breakdown curves in ammonia for different inter-electrode gap values.

the two lowest voltages belonging to the diffusion–drift branch and the highest one belonging to the Paschen branch. The diffusion–drift branch shows a well-expressed turning point with the coordinates $p = p_{\mathrm{t}}$ and $U_{\mathrm{rf}} = U_{\mathrm{t}}$. For the conditions corresponding to the turning point the amplitude of the electron displacement in the rf field is equal to one-half of the inter-electrode gap value [25], as discussed below.

The breakdown curves for gaps of $L = 15$ mm and $L = 12.5$ mm are qualitatively similar to those for $L = 25$ mm. As the gap is decreased the diffusion–drift branches are shifted to higher rf voltages and gas pressures. Consider further the breakdown curve for the gap with $L = 6$ mm. The diffusion–drift branch of this breakdown curve is much more weakly expressed than for larger gaps. For pressures below 2.5 Torr and rf voltages between 260 and 1000 V the Paschen branch is observed, and at higher rf voltages we observe the transition to the multipactor branch.

The breakdown curve for a gap of 5 mm possesses a diffusion–drift branch for pressures above 15 Torr. The Paschen branch also has a minimum (at pressures between 1.3 and 15 Torr), and at the lowest pressures a transition towards a multipactor branch is seen. We did not observe a drift–diffusion branch for a gap of 2.5 mm over the pressure range studied. We saw only the Paschen branch and, below 0.5 Torr, a multipactor branch with practically constant rf voltage for discharge ignition, independent of the gas pressure.

Now let us consider briefly the technique for determining the electron drift velocity from the breakdown curves. This is dealt with in more detail in a previous paper [25]. Consider the motion of an electron in a uniform rf electric field. The electron drift velocity when $\nu_{\mathrm{en}} \gg \omega$ (where ν_{en} is the collision rate between electrons and gas molecules and $\omega = 2\pi f$ is the angular frequency of the rf field) is given by:

$$V(t) = \frac{eE_{\mathrm{rf}}}{m\nu_{\mathrm{en}}}\cos(\omega t), \tag{1}$$

where e and m are the electron charge and mass, respectively and E_{rf} is the rf field amplitude. The amplitude of the drift velocity

$$V_{\mathrm{dr}} = \frac{eE_{\mathrm{rf}}}{m\nu_{\mathrm{en}}} \tag{2}$$

is the maximum instantaneous velocity of electrons, corresponding to the amplitude of the rf field. On integrating (1) over time we get the amplitude A of the electron displacement:

$$A = \frac{eE_{\mathrm{rf}}}{m\nu_{\mathrm{en}}\omega} = \frac{V_{\mathrm{dr}}}{\omega}. \tag{3}$$

At the turning point of the breakdown curve (corresponding to $p = p_{\mathrm{t}}$ and $U_{\mathrm{rf}} = U_{\mathrm{t}}$) the amplitude of the electron displacement is equal to half of the gap: $A = L/2$. We can understand this in the following way: when the electron oscillation becomes larger than half the electrode spacing, the electron loss rate tends to infinity, making breakdown impossible, hence defining the lowest pressure at which breakdown can occur for diffusion–drift branch. We therefore obtain a simple formula for the electron drift velocity at the turning point:

$$V_{\mathrm{dr}} = \frac{L\omega}{2} = L\pi f. \tag{4}$$

It follows from equation (4) that the value of the electron drift velocity *at the turning point* of the breakdown curve depends only on the values of the inter-electrode gap and the frequency of the rf field. At the same time there is no dependence on the gas species. Obviously, the electron drift velocity depends on the ratio of the electric field strength magnitude to the gas pressure E/p, and this dependence is different for different gases. But, at the *specific conditions (L, p, ω) corresponding to the turning point for any particular gas* the amplitude of electron oscillations is equal to $A = L/2 = V_{\mathrm{dr}}/\omega$, and the electrons will have the same drift velocity. However, the corresponding value of E/p at this point (where the corresponding drift velocity is $V_{\mathrm{dr}} = L\omega/2$) will be different for each gas.

The coordinates of the turning point permit us to determine the reduced field, E/p, corresponding to this electron drift velocity. For example, taking the coordinates of the turning point observed in the breakdown curve for a gap of 25 mm: $p_{\mathrm{t}} = 0.049$ Torr and $U_{\mathrm{t}} = 76$ V. Then $E/p = 620.4\,\mathrm{V\,cm^{-1}\,Torr^{-1}}$ and $V_{\mathrm{dr}} = 1.065 \times 10^8\,\mathrm{cm\,s^{-1}}$. Thus the measured breakdown curve for one gap value provides one value of the electron drift velocity (provided that the breakdown curve possesses a diffusion–drift branch with a well-expressed turning point).

In order to obtain a set of V_{dr} values over a wide range of E/p, rf breakdown curves must be recorded at various values of the inter-electrode gap L. The breakdown curves in the range $L \geqslant 5$ mm possess a diffusion–drift branch with a turning point (see figure 1), and can therefore be used to determine the electron drift velocity. We recorded 16 breakdown curves for different gap values in the range of $L = 5$–27 mm, thus obtaining 16 V_{dr} values in the range of $E/p = 42$–$713\,\mathrm{V\,cm^{-1}\,Torr^{-1}}$.

The values of the electron drift velocity determined from our measured breakdown curves are presented in figure 2. The same figure shows previous measurements in the literature [18, 19, 21]. However, our results cannot be compared to these, as they only concern measurements for reduced fields below $20\,\mathrm{V\,cm^{-1}\,Torr^{-1}}$, whereas our results refer to the range $E/p = 42$–$713\,\mathrm{V\,cm^{-1}\,Torr^{-1}}$. Therefore we have compared our results to calculated values derived from the cross-sections of Hayashi [27] using the Bolsig code (www.kinema.com).

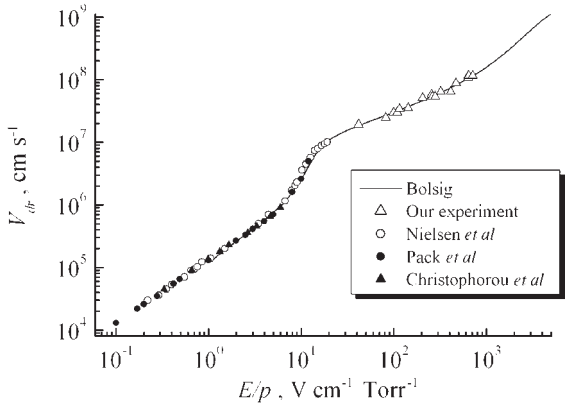

Figure 2. Electron drift velocity in ammonia against E/p. Solid curve presents the calculation data obtained with the Bolsig code, empty triangles are for our measured data, empty circles are for the experimental data from [18], solid circles are for the experimental data from [19], solid triangles are for the experimental data from [21].

4. Calculated electron transport parameters

The Bolsig code can be used to calculate electron transport parameters in the electric field in the range $E/p \geqslant 1\,\mathrm{V\,cm^{-1}\,Torr^{-1}}$ for 15 different gases and their mixtures, but does not contain ammonia. Therefore we took the cross-sections for elastic and inelastic collisions of electrons with ammonia molecules presented in the paper by Hayashi [27], added them to the set of cross-sections for this Bolsig code, extending the set of gases to 16.

Figure 2 presents the calculated values of the electron drift velocity for ammonia over the range $E/p = 1$–$5000\,\mathrm{V\,cm^{-1}\,Torr^{-1}}$ together with our measured data. It is clear that the values are in good agreement. There is also good agreement between the calculated values and the previous measurements [18, 19, 21] at low E/p.

Figure 3 shows calculated electron energy distribution functions (EEDF) for various E/p values. It is clear from the figure that a considerable change in the EEDF profile occurs for reduced fields above 6–7 $\mathrm{V\,cm^{-1}\,Torr^{-1}}$. The number of slow electrons falls and a high energy 'tail' appears. The average electron energy, $\langle\varepsilon_{\mathrm{e}}\rangle$ (figure 4) increases by almost two orders of magnitude as E/p is increased from 6 to $20\,\mathrm{V\,cm^{-1}\,Torr^{-1}}$. At the same time the electron diffusion coefficient, D_{e}, increases by three orders of magnitude, and the ratio of the diffusion coefficient to the electron mobility D_{e}/μ increases by two orders of magnitude. Although the quantities $\langle\varepsilon_{\mathrm{e}}\rangle$ and D_{e}/μ in the range $E/p < 20\,\mathrm{V\,cm^{-1}\,Torr^{-1}}$ have been published previously by Christophorou *et al* [20] their data are very close to the abscissa axis, and cannot be compared easily with our present calculations.

Hayashi [27] has published the total cross-section for ionization of NH_3 molecules in the electron energy range from threshold to 1000 eV, for the sum of all possible positive ions. At the same time Mark [29] presented measurements of the partial ionization cross-sections for the different ion products, from the ionization threshold to 180 eV. Rao and Srivastava [30] have also measured the NH_3 ionization cross-sections from threshold to 1000 eV.

Figure 5 shows the total ionization rate, obtained from the cross-sections of Hayashi [27], Mark [29]

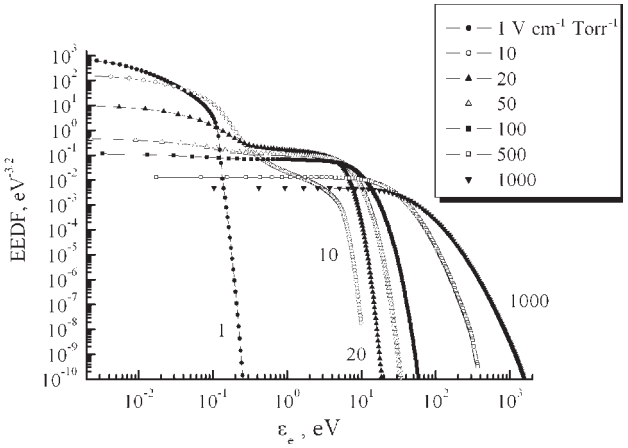

Figure 3. Electron energy distribution functions for various E/p values.

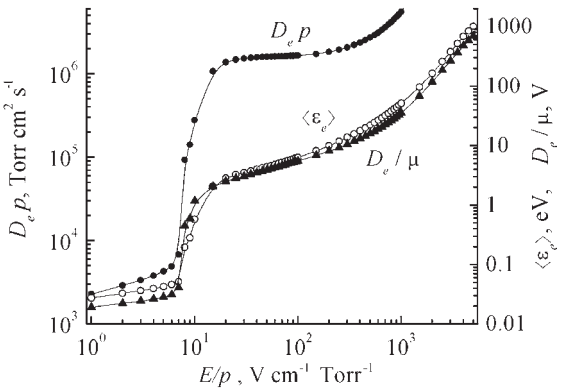

Figure 4. Electron transverse diffusion coefficient D_e, average electron energy and ratio D_e/μ against E/p.

and Rao and Srivastava [30]. In the range $E/p < 1000\,\mathrm{V\,cm^{-1}\,Torr^{-1}}$ the total ionization rates obtained from the cross-sections of Hayashi and of Mark are practically identical. However, at higher values of E/p the rate obtained from the cross-sections of Mark decreases sharply. This is probably due to the limited range of electron energy (up to 180 eV), over which Mark determined the cross-sections. In these strong electric fields, electrons can acquire energies up to hundreds of electronvolts, as can be seen in figures 3 and 4. Therefore in the range $E/p > 1000\,\mathrm{V\,cm^{-1}\,Torr^{-1}}$ the total ionization rate determined from the cross-section of Hayashi [27] should be used. At the same time it is clear from figure 5 that the total ionization rates derived from the cross-sections of Rao and Srivastava [30] for $E/p < 200\,\mathrm{V\,cm^{-1}\,Torr^{-1}}$ are considerably lower than those obtained from the other cross-sections [27, 29]. This is because their cross-sections are considerably smaller below 25 eV. However for higher E/p values the values of the total ionization frequency obtained from the cross-sections of Hayashi [27] and Rao and Srivastava [30] coincide.

Figure 6 shows the rates of electron collisions with ammonia molecules for elastic collisions, ν_{elast}, for excitation of two electronic levels, ν_{exc1} and ν_{exc2}, for excitation of three vibrational levels ν_{vibr1}, ν_{vibr2} and ν_{vibr3}, for ionization, ν_{ion} and for attachment, ν_{att}, determined from the cross-sections

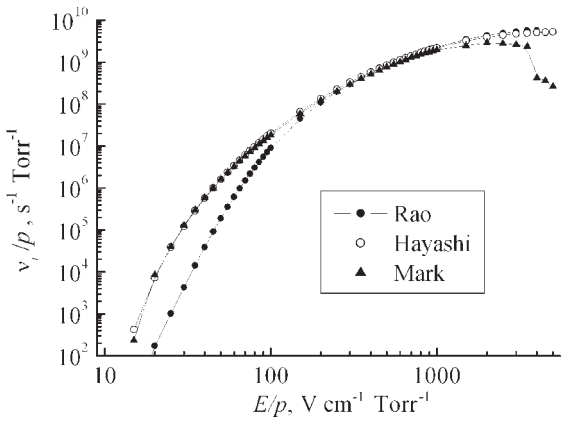

Figure 5. The total ionization frequency obtained from the cross-sections of Hayashi [27], Mark [29] and Rao and Srivastava [30] against E/p.

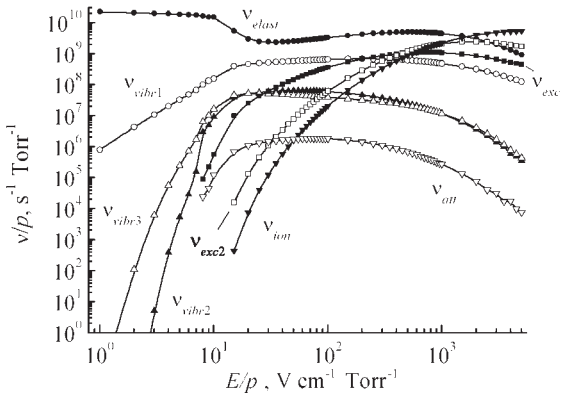

Figure 6. The frequency of elastic collisions between electrons and NH_3 molecules ν_{elast}, the frequencies of excitation of two electronic levels ν_{exc1} and ν_{exc2}, the frequency of excitation of three vibrational levels ν_{vibr1}, ν_{vibr2} and ν_{vibr3}, the ionization frequency ν_{ion} and the attachment frequency ν_{att}, determined from the cross-sections by Hayashi [27], against E/p.

by Hayashi [27]. The curves for ν_{ion} and ν_{att} cross over at $E/p \approx 50\,\mathrm{V\,cm^{-1}\,Torr^{-1}}$. We cannot compare the results of our calculations with any results of other authors.

Figure 7 presents δ, the fraction of the energy, lost by electrons as a result of collisions with ammonia molecules, against E/p. The quantity δ was determined from the elastic and inelastic collision frequencies presented in figure 6, using the formula:

$$\delta = \frac{(2m/M)\cdot \nu_{\mathrm{elast}} + \sum_{i=1}^{2} \nu_{\mathrm{exc},i} + \sum_{j=1}^{3} \nu_{\mathrm{vibr},j} + \nu_{\mathrm{ion}} + \nu_{\mathrm{att}}}{\sum \nu}, \tag{5}$$

where

$$\sum \nu = \nu_{\mathrm{elast}} + \sum_{i=1}^{2} \nu_{\mathrm{exc},i} + \sum_{j=1}^{3} \nu_{\mathrm{vibr},j} + \nu_{\mathrm{ion}} + \nu_{\mathrm{att}} \tag{6}$$

is a sum of all possible collision frequencies between electrons and molecules. The broken line in the same figure shows the quantity $2m/M$, where M is the mass of the ammonia molecule describing the quantity of energy imparted by elastic collisions. It is clear that over the whole E/p range presented in figure 7

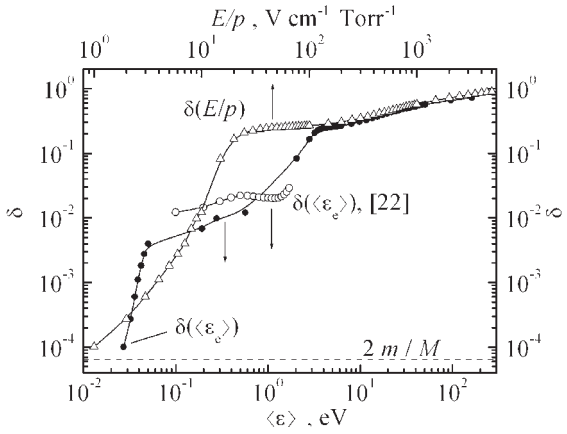

Figure 7. Portion of energy δ electrons lose on colliding with ammonia molecules against E/p and average electron energy. Empty circles are for the results of [22].

the quantity $\delta \gg 2m/M$, so that even for low E/p values the electrons can excite the vibrational levels of the ammonia molecule.

Figure 7 also shows the dependence of δ on the average electron energy $\langle\varepsilon_e\rangle$, together with published data of Christophorou and Carter [22] for average energy in the range $\langle\varepsilon_e\rangle = 0.1$–$1.7$ eV. It follows from this figure that the results of paper [22] are in reasonable agreement with our present calculated values.

5. Conclusions

We have determined the electron drift velocity in NH_3 from the location of the turning points of the breakdown curves of rf capacitive gas discharges over the range $E/p =$ 42–713 V cm^{-1} Torr^{-1}. With the help of the numerical code Bolsig and published cross-sections we have calculated the electron transport parameters (electron drift velocity, the frequencies of elastic and inelastic collisions between electrons and ammonia molecules, the electron diffusion coefficient, the average electron energy, the ratio of the diffusion coefficient to the electron mobility and the fraction of the electron energy lost on colliding with molecules) in ammonia in the range $E/p =$ 1–5000 V cm^{-1} Torr^{-1}. The values of the drift velocity obtained from our experiment are in good agreement with the calculated data.

Acknowledgment

The authors express their gratitude to the UNAXIS France—Displays Division, Palaiseau, France for their financial support and for the equipment used in this study.

References

[1] Bellakhal N 2002 *Mater. Res. Bull.* **37** 2539
[2] Dimitrova T, Atanassova E, Beshkov G and Pazov J 1994 *Thin Solid Films* **252** 89
[3] Shul R J and Pearton S J 2000 *Handbook of Advanced Plasma Processing Techniques* (Berlin: Springer)
[4] Alexandrov L N, Belousov I I and Efimov V M 1988 *Thin Solid Films* **157** 337
[5] Gupta M, Rathi V K, Singh S P and Agnihotri O P 1988 *Thin Solid Films* **164** 309
[6] Gonzalvez J M, Luna R G, Tudanca M, Sanchez O, Albella J M and Martinez-Duart J M 1992 *Thin Solid Films* **220** 311
[7] Lieberman M A and Lichtenberg A J 1994 *Principles of Plasma Discharges and Materials Processing* (New York: Wiley)
[8] Takechi K, Takagi T and Kaneko S 1998 *Japan. J. Appl. Phys.* **37** 1996
[9] Orfert M and Richter K 1999 *Surf. Coat. Technol.* **116–119** 622
[10] Ohta H, Nagashima A, Hori M and Goto T 2001 *J. Appl. Phys.* **89** 5083
[11] Gleskova H, Wagner S, Gasparik V and Kovac P 2001 *Appl. Surf. Sci.* **175–176** 12
[12] Schultz A, Baumgartner K-M, Feichtinger J, Walker M, Schumacher U, Eike A, Herz K and Kessler F 2001 *Surf. Coat. Technol.* **142–144** 771
[13] Sansonnens L, Bondkowski J, Mousel S, Schmitt J P M and Cassagne V 2003 *Thin Solid Films* **427** 21
[14] Schultz A, Feichtinger J, Kruger J, Walker M and Schumacher U 2003 *Surf. Coat. Technol.* **174–175** 947
[15] Kim B, Kim D W and Han S S 2004 *Vacuum* **72** 385
[16] Morosanu C E 1982 *Thin Solid Films* **91** 251
[17] Ron Y, Raveh A, Carmi U, Inspektor A and Avni R 1983 *Thin Solid Films* **107** 181
[18] Nielsen R A and Bradbury N E 1937 *Phys. Rev.* **51** 69
[19] Pack J L, Voshall R E and Phelps A V 1962 *Phys. Rev.* **127** 2084
[20] Christophorou L G, Datskos P G and Carter J G 1991 *Nucl. Instrum. Meth. Phys. Res.* A **309** 160
[21] Christophorou L G, Carter J G and Maxey D V 1982 *J. Chem. Phys.* **76** 2653
[22] Christophorou L G and Carter J G 1968 *Chem. Phys. Lett.* **2** 607
[23] Lisovskiy V A and Yegorenkov V D 1997 *Record-Abstracts of IEEE Int. Conf. on Plasma Science (San Diego, USA)* p 137
[24] Lisovskiy V A 1998 *Tech. Phys. Lett.* **24** 308
[25] Lisovskiy V A and Yegorenkov V D 1998 *J. Phys. D: Appl. Phys.* **31** 3349
[26] Lisovskiy V A and Yegorenkov V D 1999 *J. Phys. D: Appl. Phys.* **32** 2645
[27] Hayashi M 1990 in *Nonequilibrium Processes in Partially Ionized Gases* ed M Capitelli and J N Bardsley (New York: Plenum) p 333
[28] Levitskii S M 1957 *Sov. Phys.—Tech. Phys.* **2** 887
[29] Mark T D 1985 *Electron Impact Ionization* ed T D Mark and G H Dunn (Wien: Springer) p 137
[30] Rao M V V S and Srivastava S K 1992 *J. Phys. B: At. Mol. Opt. Phys.* **25** 2175